In-situ fatigue life prognosis for composite laminates based on stiffness degradation

Tishun Peng[1], Yongming Liu[*], Abhinav Saxena[2], and Kai Goebel[3]

[1]*School for Engineering of Matter, Transport and Energy, Arizona State University, Tempe, AZ, 85287, USA*
[2]*SGT, NASA Ames Research Center, Moffett Field, CA, 94035, USA*
[3]*NASA Ames Research Center, Moffett Field, CA, 94035, USA*

Abstract

In this paper, a real-time composite fatigue life prognosis framework is proposed. The proposed methodology combines Bayesian inference, piezoelectric sensor measurements, and a mechanical stiffness degradation model for in-situ fatigue life prediction. First, the composites stiffness degradation is introduced to account for the composites fatigue damage accumulation under cyclic loadings and a new growth rate-based stiffness degradation model is developed. Following this, the general Bayesian updating-based fatigue life prediction method is discussed. Several sources of uncertainties and the developed stiffness degradation model are included in the prognosis framework. Next, an in-situ composites fatigue testing with piezoelectric sensors is designed and performed to collected sensor signal and the global stiffness data. Signal processing techniques are implemented to extract damage diagnosis features. The detected stiffness degradation is integrated in the Bayesian inference framework for the remaining useful life (RUL) prediction. Prognosis performance on experimental data is validated using prognostics metric. Finally, some conclusions and future work are drawn based on the proposed study.

*Corresponding author:
School for Engineering of Matter, Transport and Energy, Arizona State University, Tempe, AZ, 85287-9309, USA
Tel: 480-965-6883
Fax: 480-727-9321
Email: yongming.liu@asu.edu

Key words: composites, Bayesian inference, fatigue, stiffness, prognosis, structural health monitoring

1. Introduction

The use of composite materials in engineering application has drawn extensive attention recently, which is mainly due to their better characteristics in the fatigue resistance and strength to weight ratio compared to metallic materials. Fatigue induced damage may cause serious safety concerns and/or performance degradation during long term lifetimes. In realistic applications, stress concentration are introduced at weaker sections, such as window, joints, etc., that are susceptible to delamination, matrix cracking, and fiber breakage damages. Composite specimen with notches or holes have been studied extensively to simulate these conditions in laboratory conditions [1-3]. For example, fatigue response of carbon/epoxy laminates containing circular hole was experimentally investigated and various types of laminate layup have been studied in [4, 5]. Sub-critical fatigue damage development in open-hole composite specimen were investigated both experimentally and numerically [6, 7].

Many existing studies have been done on explicitly incorporating the different types of damages (e.g. cracks, delamination) in the damage evolution model for the fatigue life prediction [6, 8-11]. The progressive damage propagation within composite-metal interface or post-buckled laminates has been investigated in [12-15] , in which new interface elements are developed to capture the cohesive behavior of delamination growth under fatigue loading. Majority of these methods are based on finite element method (FEM), which focuses on the mechanisms investigation and modeling. In-situ fatigue life prognosis that directly uses these models will be very difficult due to the computational complexity. In addition, the diagnosis and quantification of various types of damages in-situ is a challenging problem, which makes the prediction based

on the high fidelity FEM model very difficult. Some researchers use an alternative approach for life prediction at the macro level, which is based on the strength or stiffness degradation induced by fatigue loading [16-21]. Whitworth [20] proposed a statistical model that describes the residual stiffness using a two-parameter Weibull distribution. In [21], a normal distribution was proposed to predict the residual stiffness of composite laminates. In both approaches, the residual stiffness model ignores the effect of applied stress which is generally not true for fatigue problems. Shirazi and Varvani-Farahani [22] proposed to use the stiffness degradation to develop a fatigue damage model for a unidirectional fiber-reinforce polymer (FRP) laminates system. A relationship between the stiffness reduction and the remaining fatigue life ratio was developed. This model is relatively difficult for the in-situ fatigue prediction because the field measurements for stiffness are very difficult and the knowledge of ultimate fatigue life is not available beforehand. Unlike the stiffness measurement in the library conditions, it is difficult to obtain stiffness reduction measurements directly under service conditions. Thus, it would be desirable if the stiffness degradation can be inferred using a feasible structural health monitoring system. Lamb wave-based damage detection methods are more widely used [23, 24] for structural health monitoring because of their low cost and high efficiency [25]. Lamb waves can propagate in thin plate without too much dispersion in certain modes [26]. Based on the fact that Lamb wave propagation is highly dependent on material stiffness, it is expected that stiffness degradation will be captured by the received Lamb wave signal propagating through the specimen. Since piezoelectric sensors are embedded in the structure, system health can be measured in-situ on a continuous basis, which lays foundation for more effective RUL prognosis.

Based on the above brief review, the proposed study tries to develop a macro level stiffness degradation model that can be used for in-situ fatigue life prediction at different stress levels.

Two major components are required for the proposed study: 1) a stiffness degradation model that depends on the different loading conditions and correlates with the fatigue life; 2) in-situ measurements of stiffness degradation that can provide current damage state for the remaining life prediction. This paper is organized as follows. First, a growth rate-based stiffness degradation model is proposed to express the stiffness evolution kinetics under different constant amplitude loading. Next, a general Bayesian inference framework is discussed for real time fatigue life prognosis using the developed stiffness degradation model with in-situ measurements. Following this, a Lamb wave-based fatigue testing setup is given, in which both sensor signal and true stiffness degradation measurements are collected periodically. A diagnosis model for stiffness estimation using measured piezoelectric sensor signal is discussed and is incorporated in the Bayesian prognosis framework. Model verification and validation is performed using experimental measurements to show the performance of the proposed approach.

2. Stiffness degradation model development

In this section, a general model for composites stiffness degradation is proposed. The key idea is to express the overall composites stiffness reduction at certain loading cycles using a growth rate kinetics. The proposed model is analogous to the well-known Paris' law for the fatigue crack growth approach. The aim is to study the composites damage progression at the tensile-tensile stage. Thus, the experimental design used the stress range and stress ratio as the controlling parameters. This experimental design is different than the classical S-N curve testing for composite materials, which uses the stress range and mean stress as the controlling parameters. With fixed stress ratio, the stiffness degradation rate is assumed to be a function of the applied stress range and the current stiffness value. Detailed the discussion is given below.

Under fatigue loadings, different forms of damage such as matrix cracking, delamination and fiber breaking will occur simultaneously or sequentially, which will eventually lead to the final failure of the entire composite component. The concept of the stiffness degradation-based life prediction is to implicitly incorporate different forms of damage mechanism into different stages stiffness degradation curve. A schematic representation of a general stiffness degradation curve for composites is shown in Fig. 1.

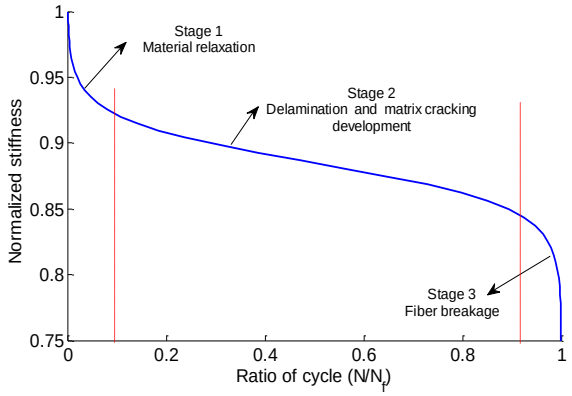

Fig. 1. The general trend for composite stiffness degradation

As shown in Fig. 1, the *x-axis* is the normalized fatigue life (i.e., normalized with respect to the final failure life) and the *y-axis* is the normalized stiffness (i.e., normalized with the stiffness before the fatigue loading). The stiffness degradation process can be divided into three distinct stages. Initially, the stiffness decrease quickly during initial loading stage. In this stage, some initial defect in the material will quickly approaches to the stable stage. After that, the stiffness decreases gradually due to the development of delamination and matrix cracking. Close to the final failure state, the stiffness drops dramatically because of the fatigue loading induced fiber breakage. The last stage is usually unstable and the specimen will fail in a very short amount of cycles.

In the experimental testing shown later, the initial relaxation state will stabilize within several hundreds to a few thousands cycles which is very small portion of the entire fatigue life span of composites under high cycle fatigue conditions. Ignoring the initial relaxation stage will not produce large error for the final fatigue life prediction. Thus, the proposed study will focus on the second and third stages, which can simplify the stiffness degradation model without sacrificing life prediction accuracy. In the proposed stiffness degradation model, two major hypotheses are made. First, the stiffness degradation rate is increasing monotonically and reaches its maximum at final failure stage. Second, for the same material, the stiffness degradation rate is assumed to be a function of the applied stress and the current stiffness. Based on the above assumptions, the generalized stiffness degradation model can be proposed as

$$\frac{\mathbf{ds}}{\mathbf{dN}} = -\mathbf{f}(\Delta\boldsymbol{\sigma}, \mathbf{s}) \tag{1}$$

where $\Delta\sigma$ is the applied stress range. s is the current normalized stiffness, which is obtained by dividing the current stiffness under health condition. N is the fatigue cycles and $\frac{ds}{dN}$ is the stiffness degradation rate during one cycle. f is a generic function which describes the relationship between the stiffness degradation rate, the stress range, and stiffness. In the proposed study, a power law function is used to represent the general trend for the second and third stage of the stiffness degradation curve. Thus, the proposed stiffness degradation model is expressed as

$$\frac{\mathbf{ds}}{\mathbf{dN}} = -\mathbf{C}(\Delta\boldsymbol{\sigma}\mathbf{s}^{-\mathbf{r}})^{\mathbf{m}} \tag{2}$$

where $\boldsymbol{C}, \boldsymbol{r}$ and $\boldsymbol{m}$ are model parameters which are assumed to be positive and can be calibrated using experimental datasets. Using Eq. (16), the predicted stiffness for given fatigue cycles can be calculated by integrating both sides as

$$\int_{\mathbf{s_0}}^{\mathbf{s}} \mathbf{s}^{\mathbf{rm}}\, \boldsymbol{ds} = \int_{\mathbf{0}}^{\mathbf{N}} -\mathbf{c}(\Delta\boldsymbol{\sigma})^{\boldsymbol{m}}\ \mathbf{dN} \tag{3}$$

In the fatigue life prognosis, the model proposed above is used to determine the system degradation under fatigue loading. Once the system response (e.g. stiffness) is available, the model parameter and uncertainties can be updated to achieve more effective prediction. One method to incorporate the stiffness measurement for the life prediction updating is the Bayesian inference method, which is discussed below.

3. Fatigue life prognosis using Bayesian inference

Remaining useful life prognosis for a structural component should be continuously updated using the latest measurement information. New information should be incorporated to improve prognostics algorithm by updating model parameters, their distributions, correcting for model errors, and updating future loading conditions. Widely used Bayes' theorem [27-29] allows updating of the parameter distributions based on the condition monitoring data from the system. A posterior distribution of the parameters can be obtained by combining its prior information and the current system response. Specifically, assume $\boldsymbol{\theta}$ is the vector of parameters of interest, which are considered as random variables and will be updated using the evidence from the monitored data d. Then the posterior distribution of these parameters can be expressed as

$$\boldsymbol{q}(\boldsymbol{\theta}|\boldsymbol{x}') \propto \boldsymbol{p}(\boldsymbol{\theta})\boldsymbol{p}(\boldsymbol{x}'|\boldsymbol{\theta}) \quad \textbf{(4)}$$

where $\mathrm{p}(x'|\boldsymbol{\theta})$ is the likelihood function, which reflects possibility of detected specimen stiffness x' given parameters $\boldsymbol{\theta}$, and $q(\boldsymbol{\theta}|x')$ is the posterior distribution of updated parameters. In our formulation, x' is normalized stiffness measured in-situ, which is usually inferred indirectly from sensor measurements. Furthermore, the stiffness inference (e.g., the diagnosis model) itself introduces additional uncertainties [30]. Therefore, it is necessary to account for measurement noise ϵ introduced by inference model and physics model uncertainty τ in the estimation. In our formulation, the relationship between x' and $M(\boldsymbol{\theta})$ is expressed as

$$\boldsymbol{x' = M(\theta) + \epsilon + \tau} \quad \textbf{(5)}$$

Assuming that the two error terms ϵ and τ are independent zero mean normal variables [31, 32], the sum of them can also be expressed as a random variable $e = (\epsilon + \tau) \sim N(0, \sigma_e)$. Therefore, the likelihood function $p(x'|\boldsymbol{\theta})$ can be expressed as

$$\boldsymbol{p(x'_1, x'_2, \ldots x'_n|\theta) = \frac{1}{(\sqrt{2\pi}\sigma_e)^n} exp\left(-\frac{1}{2}\sum_{i=1}^{n}\left(\frac{(x'_i - M(\theta))}{\sigma_e}\right)^2\right)} \quad \textbf{(6)}$$

where n is the number of available measurements. Substituting Eq.(6) into Eq.(4), the posterior distribution of parameter $\boldsymbol{\theta}$ can be expressed as

$$\boldsymbol{p(\theta|x'_1, x'_2, \ldots x'_n) \propto p(\theta) \frac{1}{(\sqrt{2\pi}\sigma_e)^n} exp\left(-\frac{1}{2}\sum_{i=1}^{n}\left(\frac{(x'_i - M(\theta))}{\sigma_e}\right)^2\right)} \quad \textbf{(7)}$$

Then the posterior distribution of the parameter $\boldsymbol{\theta}$ can be approximated by the samples drawn by the Markov Chain Monte Carlo (MCMC) simulation. Detailed discussion on the MCMC method can be found in many references [33-36] and is, therefore, not discussed here. The efficiency of the method depends on the MCMC sampling algorithm and the complexity of the stiffness degradation model used in the Bayesian inference. A simplified analytical degradation model proposed in section 2 is used in the proposed method, which makes the computation very efficient. If expensive stiffness degradation simulation model is used, e.g., finite element method-based degradation model, the computation will be more expensive.

Based on above discussions, the general framework for the in-situ fatigue life prognosis framework is given below,

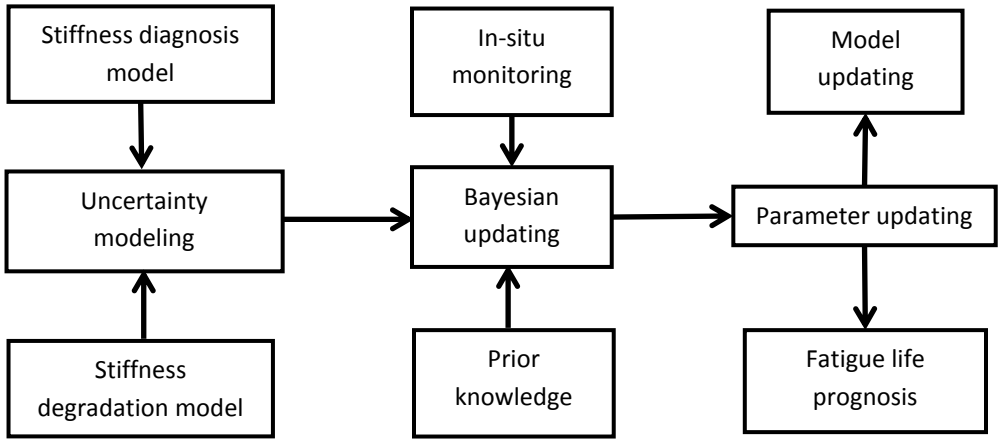

Fig. 2. The general framework for in-situ fatigue life prognosis

4. In-situ stiffness diagnosis using Lamb waves

In this section, the stiffness degradation model proposed in section 2 will be calibrated using laboratory composites fatigue experiment data. With embedded PZT sensor network system, the stiffness is estimated using the extracted damage features from digital signal processing.

4.1 Experiment Setup

The test setup for stiffness diagnosis of open-hole composites includes two major systems: data acquisition system and fatigue testing system (Fig. 3). Data acquisition system is used to generate exciting signal to the PZT sensor network and to collect the signal received by sensors. The specimen is subject to tensile-tensile constant loading spectrum using fatigue testing system. Loads with different stress amplitude are applied for different specimen. For all fatigue tests in the current study, stress ratio is fixed to be 0.1.

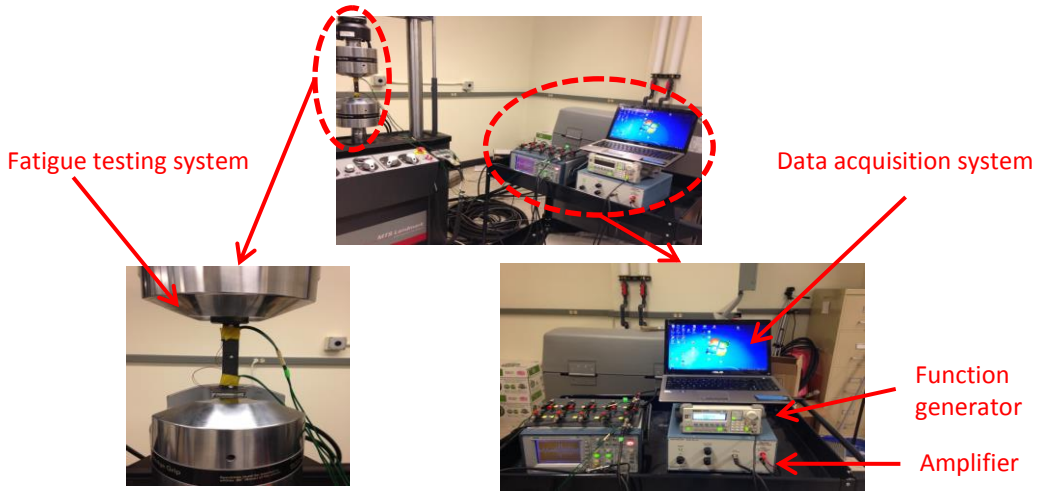

Fig. 3. Open-hole fatigue testing setup

The composite open-hole specimen is made of 12 plies of composite lamina with layup $[90_3/0_3]_s$. The raw material for manufacturing the composites is carbon fiber cloth, resin, hardener and other consuming materials, such as nylon membrane and cloth. The fiber is unidirectional carbon fiber, the resin is resin epoxy system FS-A23, Part(A) and the hardener is

epoxy system FS-B412, Part(B). All of them are produced by Fiberglast.com. The composite layup is conducted manually, and then applied with 160Mpa pressure under 100 Celsius. The schematic layup before the hot pressing is shown in Fig. 4. The specimen thickness and width varies slightly due to manufacturing variability. The nominal specimen dimension is 200x20x2 mm with a center hole diameter of 5 mm. The nominal specimen geometry is schematically shown in Fig. 5. Actuators and sensors are mounted on both sides of the open-hole specimen to add redundancy to the measurement system. Actuator 1 and sensor 1 are mounted on the front side; actuator 2 and sensor 2 are mounted on the back side of the specimen. Each actuator and sensor pair forms a diagnosis path. In the current study, the diagnosis path is used to investigate stiffness degradation along the loading direction for layup $[90_3/0_3]_s$. The proposed stiffness degradation model appears to be able capture the general degradation trend for most $(0/\theta)$ composite laminates [22]. Additional experimental studies and theoretical work are required for arbitrary composite layups.

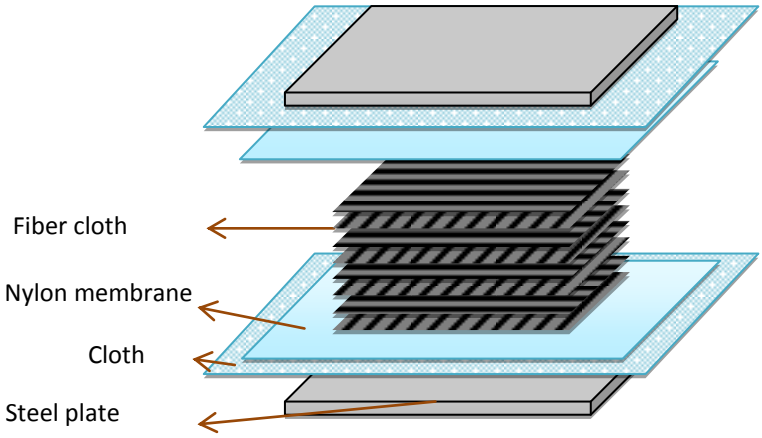

Fig. 4. Schematic representation of composite layup

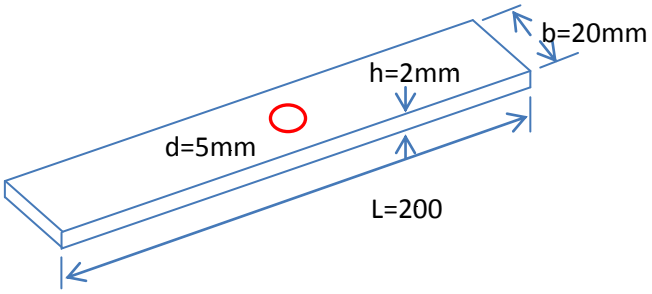

Fig. 5. The nominal geometry for the open-hole specimen

4.2 Experimental results and diagnosis model development

In this study, a hamming-windowed sinusoidal tone burst with 3.5 cycles is used as the actuating signal. Central frequency of this signal is set to be 200kHz, as shown in Fig. 6. Under fatigue loading, initially matrix cracking starts to appear in 90° plies, and then delamination follows and grows between 0° and 90° plies with fiber breaking at the same time. Most specimen fails near the center hole location. Some specimen fails at the other locations due to the splitting of the laminates. The final failure for some open-hole specimen is shown in Fig. 7.

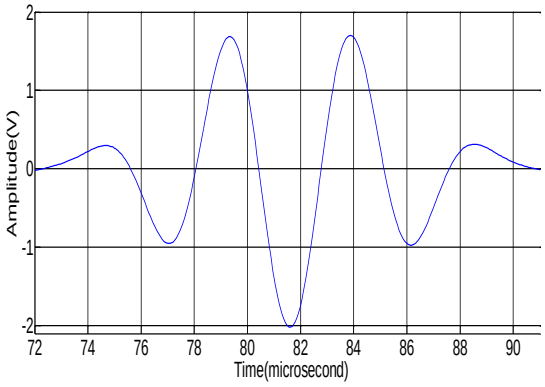

Fig. 6. A tone burst signal of 3.5 cycles with 200kHz central frequency

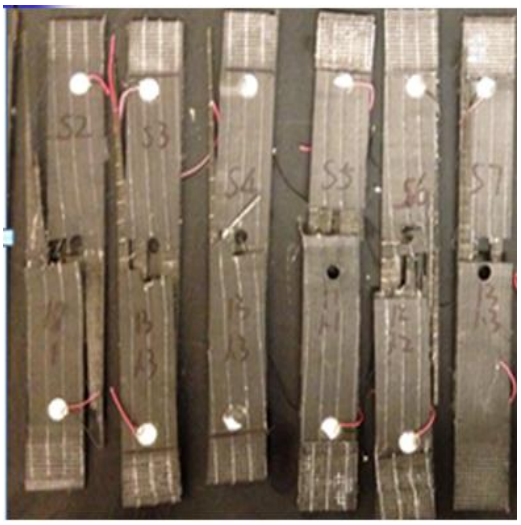

Fig. 7. The final failure pattern for open-hole specimen

After installing the specimen on the hydraulic machine, a baseline PZT signal under pristine condition is collected first. Subsequent data are collected periodically during fatigue loading cycles. The PZT signals are collected by pausing the loading machine and holding a constant load on the specimen. Band-pass filter are used to eliminate the environmental low and high frequency noises [37]. Fig. 8 illustrates a typical signal obtained for specimen S2 with a 13kN maximum force. Fig. 8(a) is the overall raw signals collected during the testing. Fig. 8(b) shows the first time-window of interest between the dashed lines in the Fig. 8(a). With further signal processing, changes in selected features, such as normalized amplitude, correlation coefficient, and cross correlation are calculated. All of these feature changes can be obtained by comparing the received signals under pristine and damage conditions. Normalized amplitude change reflects the energy dissipation due to the damage and correlation coefficient change reflects the first time window signal perturbation due to the new waves generated at the delamination or matrix cracking [37] . Cross correlation measures the similarity between these two time series. For the cross correlation at different time lags, the maximum value is extracted and normalized with respect to the maximum value under pristine condition. Specimen stiffness is measured using the force-displacement curve from the hydraulic machine output. Multiple specimen are tested here to assess reproducibility of the diagnosis method and investigate the effect of variability among different specimen. A detailed experiment summary for these specimen is provided in Table 1. To compare with different specimen under different stress range, the extracted features and

specimen stiffness are normalized with respect to their maximum value under pristine conditions. Normalized stiffness vs. different sensor signal features for different specimen is shown in Fig. 9.

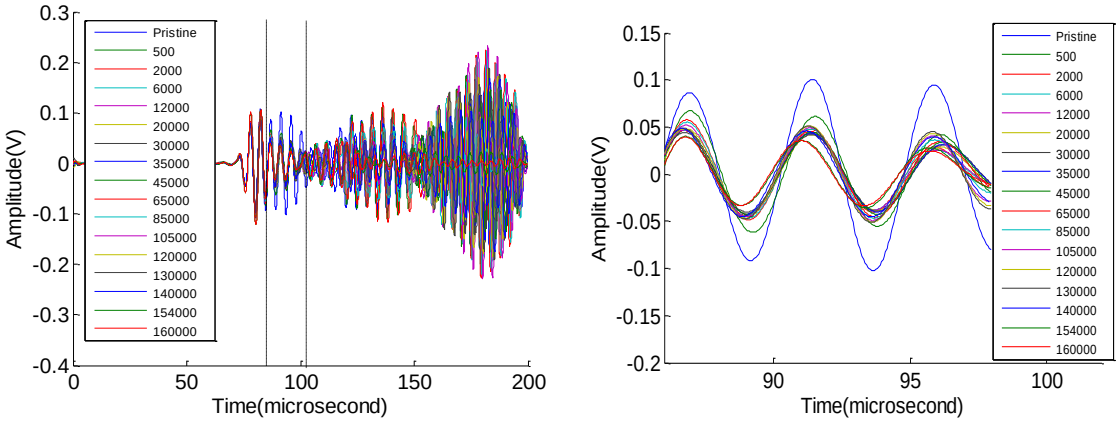

Fig. 8. The received signal for specimen S2 at different cycles

Table 1. Testing information summary for different specimen

Specimen #	Max stress (Mpa)	Stress ratio	Fatigue life (cycles)
S1	296	0.1	423500
S2	325	0.1	163400
S3	326	0.1	85600
S4	428	0.1	10680
S5	410	0.1	45000
S6	379	0.1	41257

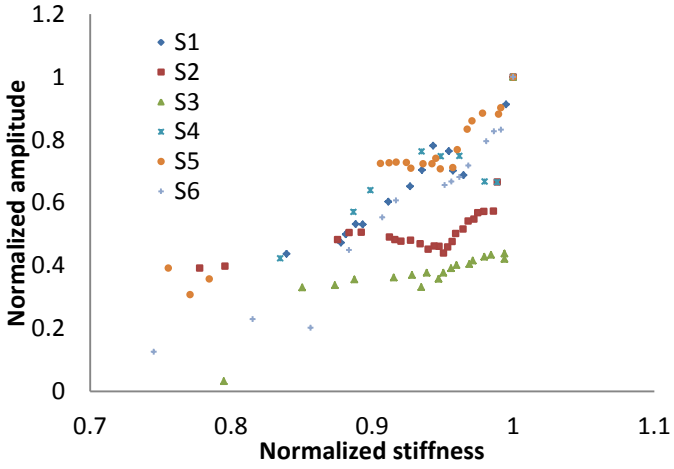

(a)

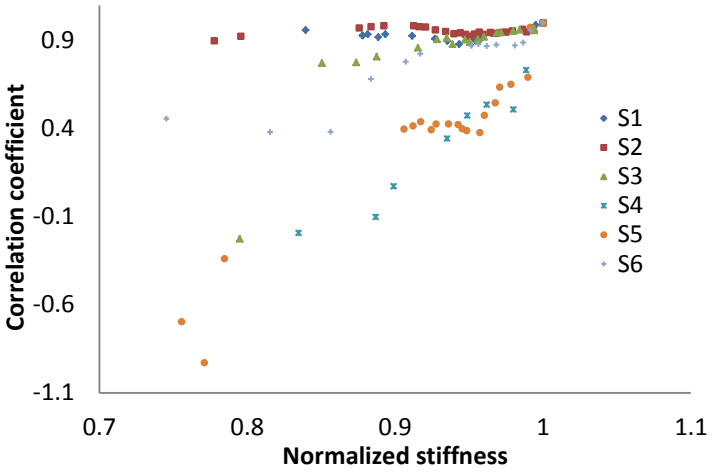

(b)

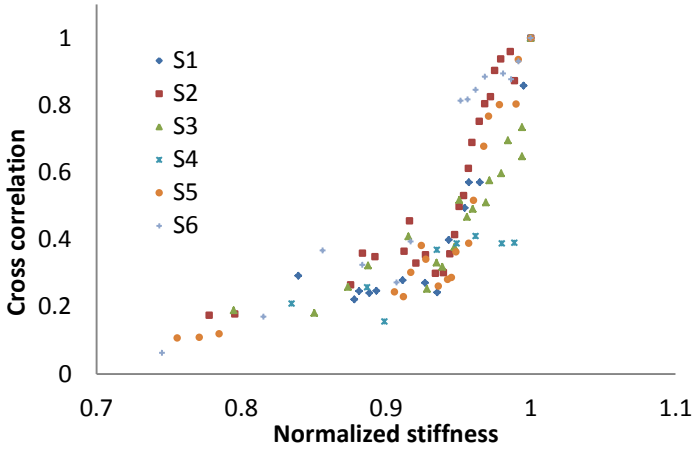

(c)

Fig. 9. These three features vs. normalized stiffness for six specimen

As seen in the above figures, large uncertainties are observed across different specimen. It is observed that these three features have generally monotonic relationship with the normalized stiffness. However, it is difficult to predict the normalized stiffness using a single feature due to the large uncertainties in different specimen. Thus, all features are combined into a second order multiple variable regression model to estimate the normalized stiffness. Collected sensor data from specimen (S1, S2, S3, S4, and S5) are used as calibration to get the regression coefficients in Eq.(8). Values for those coefficients in Eq.(8) are listed in Table 2. Sensor data from specimen

S6 is used as validation. Fig. 10 shows the predicted normalized stiffness using the proposed second order regression model.

$$s = \alpha_0 + \alpha_1 x + \alpha_2 y + \alpha_3 z + \alpha_4 x^2 + \alpha_5 y^2 + \alpha_6 \sqrt{z} + \alpha_7 xy + \alpha_8 x\sqrt{z} + \alpha_9 y\sqrt{z} \quad (8)$$

s: normalized stiffness
x: normalized amplitude
y: correlation coefficient
z: cross correlation

Table 2. Coefficients for the second order multivariate regression model

Coefficient	Value
α_0	0.5108
α_1	0.0919
α_2	-0.0440
α_3	-0.5370
α_4	0.2938
α_5	-0.0250
α_6	0.9516
α_7	-0.1060
α_8	-0.4040
α_9	0. 2675

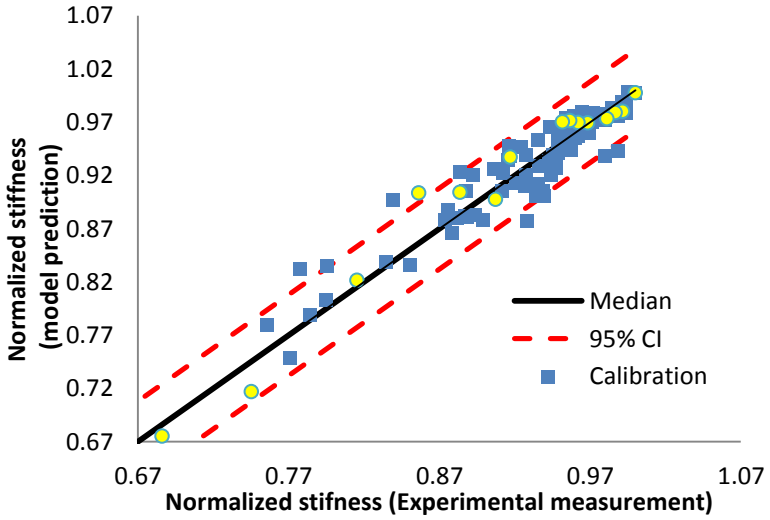

Fig. 10. The predicted normalized stiffness vs. experimental measurements (R^2=0.8819)

From Fig. 10 above, it can be seen that the proposed model can provide reasonable prediction for the normalized stiffness. The predicted normalized stiffness for specimen S6 will be used in the following section as a demonstration example for RUL prediction.

4.3 Probability of detection

The probability of detection (PoD) measures the detection capability of Non-destructive technique (NDT) under certain inspection conditions [38]. As discussed above, the system response (i.e. the stiffness degradation) is estimated using ultrasonic signal features. The PoD of the diagnosis model is derived and presented in detailed below. Assume $\hat{s}$ is the detected normalized stiffness and s is the true system response of interest, then the PoD curve for these data can be approximated using linear relationship between $\ln(\hat{s})$ and $\ln(s)$ [38], which is expressed as,

$$\mathbf{\ln(\hat{s}) = \beta_0 + \beta_1 \ln(s) + \delta} \tag{9}$$

where δ is an error term, which is normally distributed with zero mean and standard deviation σ_δ, β_0 and β_1 are model coefficients. In this problem, the normalized stiffness will be considered as detected if $\hat{s}$ is less than the pre-specified threshold s_{th}. Therefore, the function PoD(s) can be given as,

$$\mathbf{PoD(s) = P(\ln(\hat{s}) < \ln(s_{th})) = 1 - \Phi((\ln(s) - \mu)/\sigma)} \tag{10}$$

$$\mathbf{\mu = (\ln(s_{th}) - \beta_0)/\beta_1} \tag{11}$$

$$\mathbf{\sigma = \sigma_\delta/\beta_1} \tag{12}$$

where Φ is the cumulative distribution function of the standard normal distribution. Given the detected $\hat{s}$ and available true system response s, the coefficients in Eq. (9) can be estimated using linear regression, which is expressed as,

$$\mathbf{\ln(\hat{s}) = -0.0096 + 0.8465 \ln(s) + \delta} \tag{13}$$

where δ is the error term. In order to validate the distribution of δ, its histogram and normal probability paper are shown in Fig. 11.

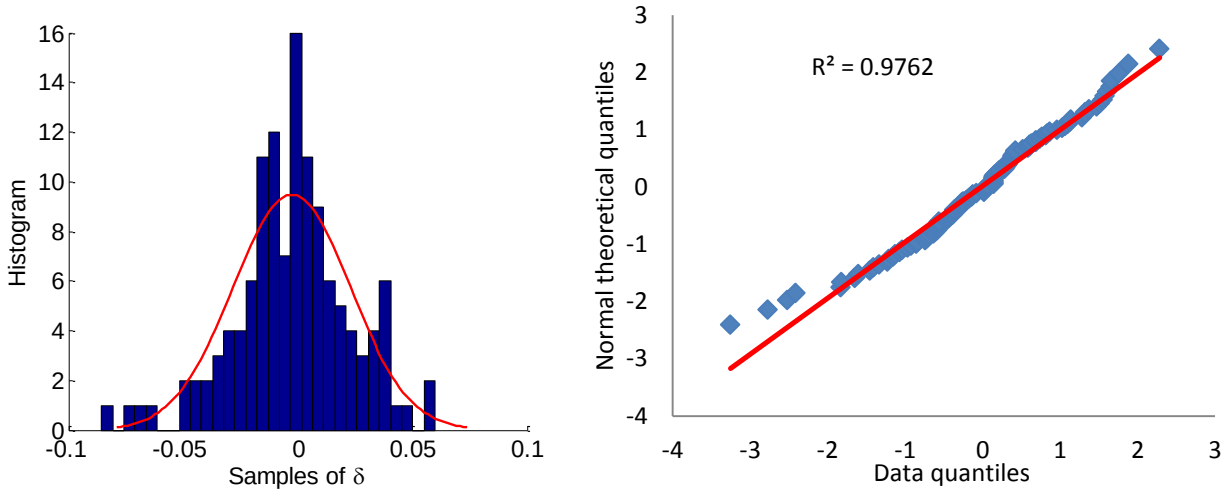

Fig. 11. The histogram and probability plot of term δ

From Fig. 11, it can be observed that the probability plot shows highly linear trend based on the linear regression statistics, which also substantiates that the error term is normally distributed. Observation from the data suggests that the normalized stiffness can be detected once it is less than *1*, thus the pre-specified threshold s_{th} is set to be *1*. With above information, the parameter μ and σ can be calculated as,

$$\boldsymbol{\mu = \frac{\ln(s_{th}) - \beta_0}{\beta_1} = \frac{\ln(1) - (-0.0096)}{0.8465} = 0.0113} \quad \textbf{(14)}$$

$$\boldsymbol{\sigma = \frac{\sigma_\delta}{\beta_1} = \frac{0.0255}{0.8465} = 0.0301} \quad \textbf{(15)}$$

Using Eq. (10), the PoD for different normalized stiffness is illustrated below in Fig. 12. It can be seen that over 90% PoD can be achieved when normalized stiffness is less than 0.97. It demonstrates the accuracy and sensitivity of the proposed detection method for stiffness degradation.

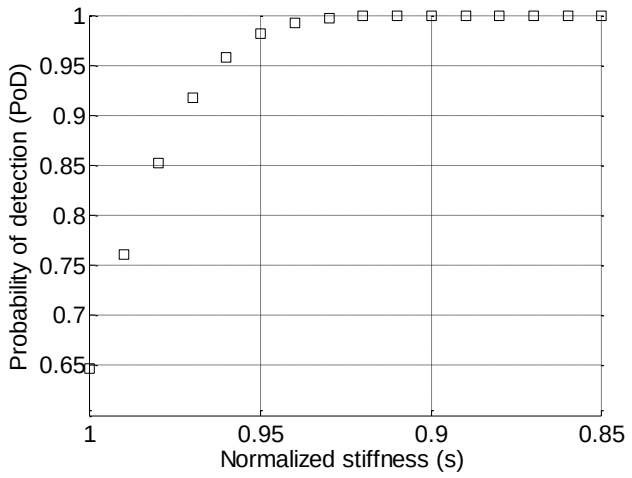

Fig. 12. The histogram and probability plot of term δ

4.4 Stiffness degradation model validation

To validate the general stiffness degradation trend shown in Fig. 1, measured stiffness degradation curves for all the specimen are shown in Fig. 13. In order to get the kinetics equation for the stiffness degradation, local time derivatives (i.e., rate) are required. To get a smooth estimation for local derivatives, 5 point local polynomial regression is used [39]. The stiffness changing rate per cycle is shown in Fig. 13.

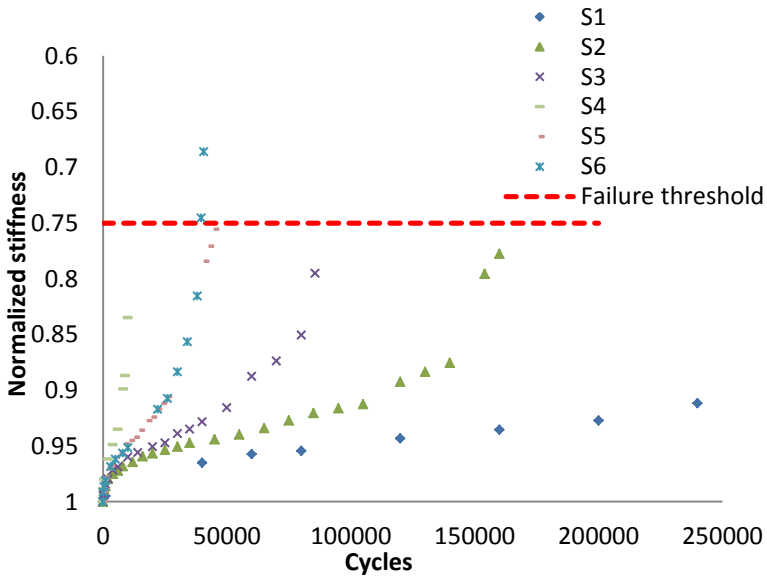

Fig. 13. The stiffness degradation curves for all specimen

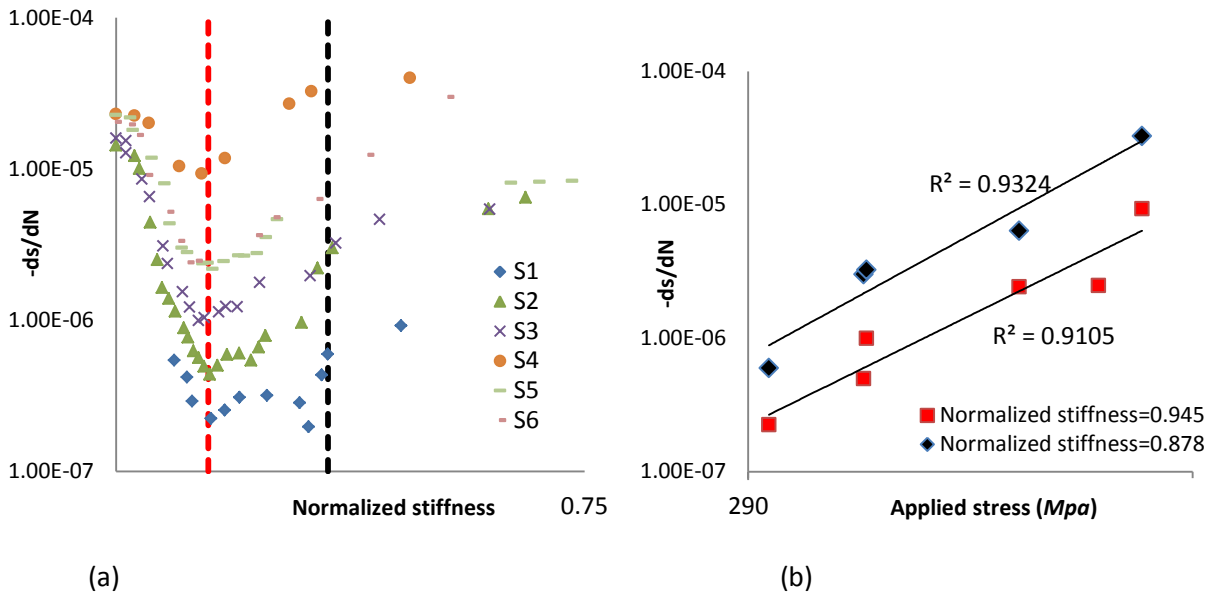

Fig. 14. The stiffness degradation rate for different specimen (Log-log scale).

(a), Versus normalized stiffness. (b), Versus applied stress

From Fig. 14, it can be observed that normalized stiffness decreases very fast at the initial stage and so does the stiffness degradation rate. The degradation rate reaches its minimum at the transition point from stage 1 to stage 2 shown as red dashed line in Fig. 14(a). During stage 2, the degradation rate is increasing gradually and reaching to its maximum at its final failure stage. Fig. 14 indicates that the stiffness degradation rate is log-linear with respect to the current normalized stiffness value and applied stress. The stiffness degradation rate is plotted with respect to a mixed stiffness and stress term in Fig. 15.

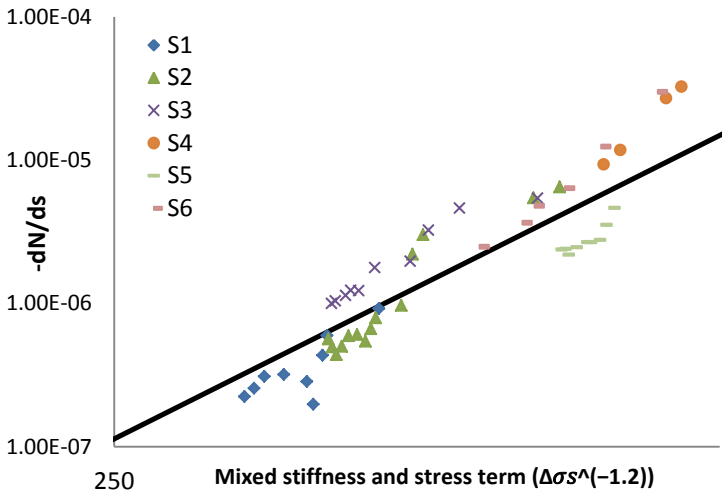

Fig. 15. The stiffness degradation rate considering the applied stress(Log-log scale)

From Fig. 15, all the curves coalesce and form a general linear relationship can be obtained between the stiffness degradation rate and the term of $\Delta\sigma s^{-1.2}$ in log-scale. Based on that, the proposed stiffness degradation model is calibrated as,

$$\mathbf{ds/dN} = -\mathbf{C}(\Delta\boldsymbol{\sigma s}^{-1.2})^{\boldsymbol{m}} \quad \textbf{(16)}$$

where N is the fatigue cycle at time t, s is the normalized stiffness, C and m are model parameters, which may vary for different specimen. These two parameters will be considered as random variables so as to capture the uncertainties between different specimen. There distributions will be updated using the proposed Bayesian inference framework. A demonstration example will be given in the following section.

5. Demonstration example

Following the framework shown in Fig. 2, the stiffness degradation model and diagnosis model proposed above are integrated using Bayesian inference for fatigue life prognosis. In the stiffness degradation shown in Eq.(3), the lower integration limit S_0 should be determined initially in order to obtain the predicted stiffness at cycle N. Due to ignorance of the initial stage of stiffness degradation. The parameter S_0 is approximated with initial stage stiffness degradation data obtained from all specimen. The value is around 0.99 for all specimen. The prior distribution of

parameters C and m are determined by the linear regression statistics illustrated in Table 3. In this study, the normalized stiffness is inferred from piezoelectric sensor signal and is estimated using the quadratic regression model given in Eq.(8) . The failure threshold is set to be 0.75, because it is within the final failure stage for all specimen. When the stiffness degradation reaches 0.75 of the original stiffness, the degradation rate becomes very fast and specimen fails after only a few to few hundred cycles. The remaining life of the specimen after reaching 0.75 is less than 3% of the entire life for the current investigation. It should be noted that the threshold should depend on the layups as the failure mechanisms will be different for different layups. Detailed and quantitative study requires significant amount of experimental and theoretical work in the future.

Predictions using the proposed diagnosis and prognosis framework and the experimentally measured stiffness and life are compared together in Fig. 16-17. In Fig. 16-17, the x-axis is the fatigue cycles and the y-axis is the normalized stiffness. The measured stiffness using hydraulic machine (ground truth), the inferred stiffness from piezoelectric sensor signal (diagnosis), and the Bayesian updating results (prognosis) are shown together. Fig. 16 shows the predictions with prior distribution of parameters. The prior distributions for the two parameters are listed in Table 3. As can be seen, the prior distribution of parameters are from other testing specimen data and is very different from the investigated specimen. Thus, a large error is observed for the prediction of stiffness degradation and life (i.e., the fatigue cycles when the unstable stiffness degradation occurs). Fig. 17 shows the updated results from the proposed prognosis method with different numbers of observation points. Blue solid line is the median prediction using the prior distribution. Hollow rectangular points are the experimentally measured stiffness. Black solid points are the stiffness inferred from the Lamb wave-based damage detection method.

Table 3. The prior distribution of two model parameters

Parameter	C	m
PDF	Log-normal	normal
Mean	-60	8.3

Standard deviation	0.2	0.1

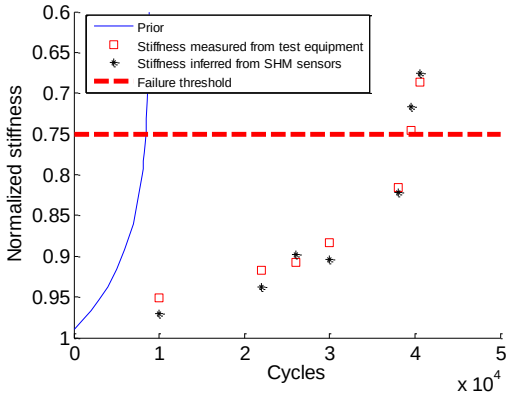

Fig. 16. The prior belief and experimental datasets

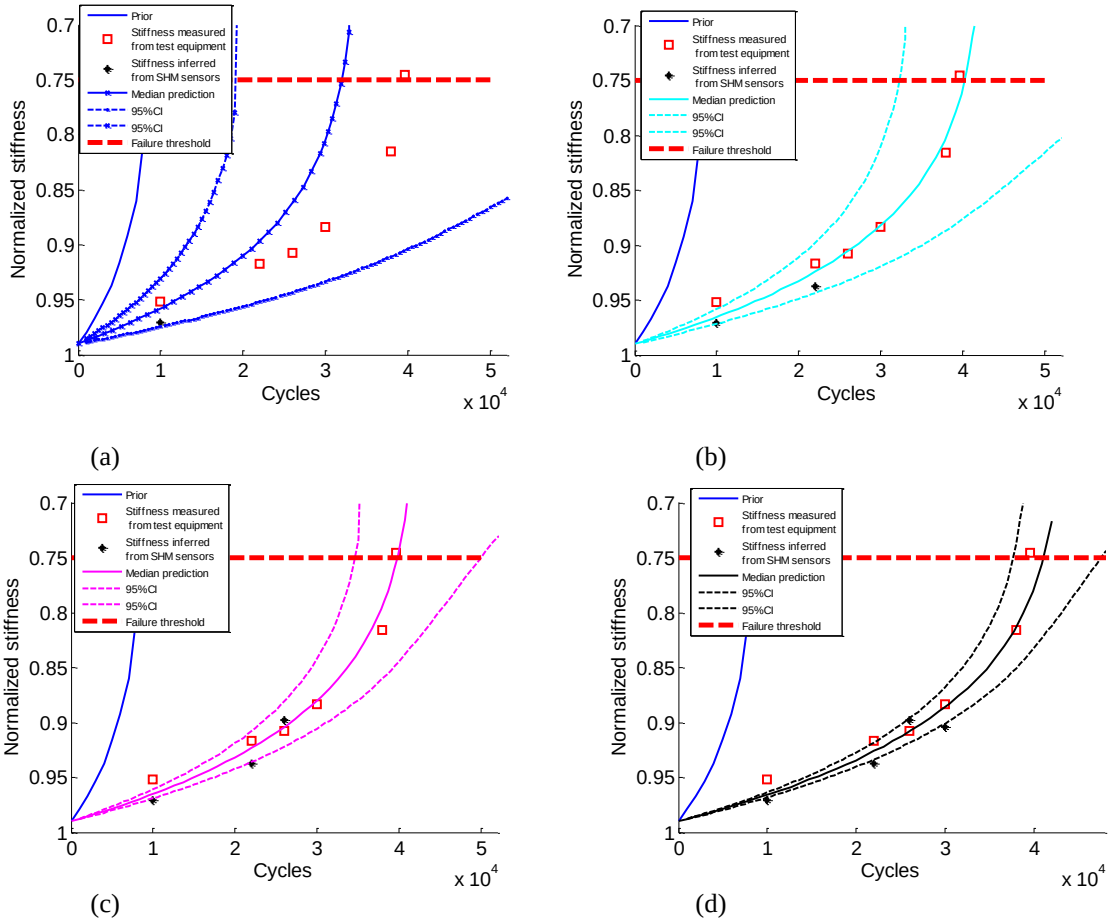

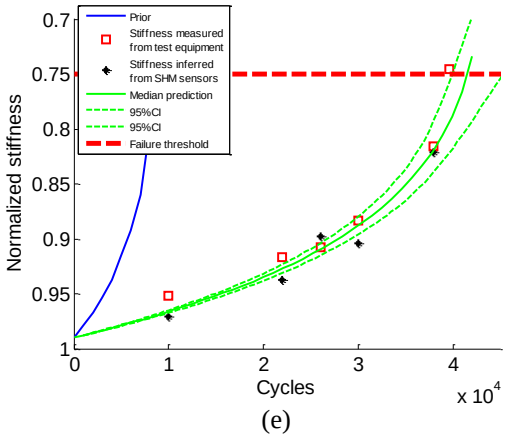

Fig. 17. Bayesian updating result. (a) Updating one, (b) updating two, (c) updating three, (d), updating four, and (e) updating five.

From Fig. 17, it can also be seen that the median prediction trend gets closer to the experimentally measured ground truth with additional updating using inferred stiffness data. The uncertainty bounds become narrower with additional updating, which indicates the effectiveness of the Bayesian updating method in reducing prognostic uncertainties. This trend can also be observed in the updated parameter distribution, shown in Fig. 18.

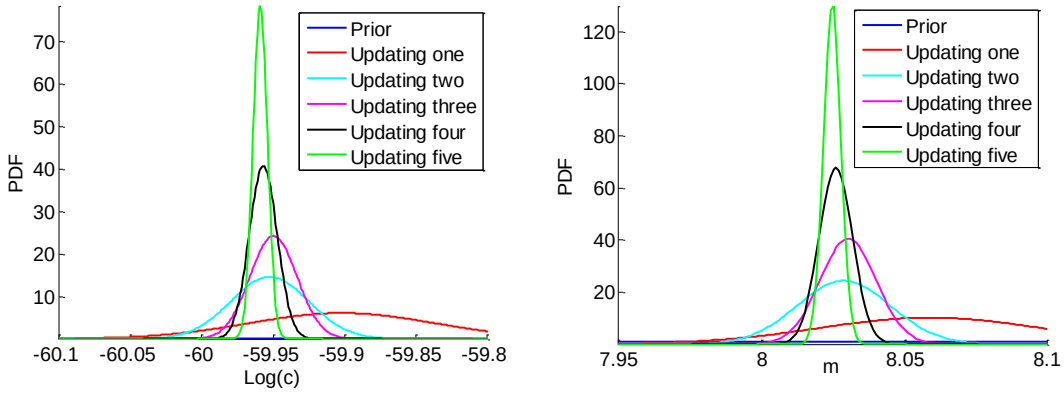

Fig. 18. Parameters updating result. (a), updated Log(c), (b), updated m

To evaluate the performance of the prognostic model, prognostic metrics are employed. A detailed discussion of metrics-based model validation can be found in [40-43]. Several relevant metrics, such as Prognostic Horizon (PH), $\alpha - \lambda$ Accuracy, Relative Accuracy (RA), Cumulative Relative Accuracy (CRA), and Convergence are discussed in that publication. In this paper,

Prognostic Horizon is used to assess prognostic algorithms performance. The Prognostic Horizon describes the length of time before end–of–life (EoL) when a prognostic algorithm starts predicting with desired accuracy limits. The limit is expressed using an α-bound given by $\pm\alpha \cdot t_{EoF}$. In contrast, $\alpha - \lambda$ Accuracy determines whether prediction accuracy is within desired accuracy levels (specified by α) around RUL at any given time specified by λ. The smaller α means the higher desired accuracy. The performance is visually depicted on an RUL vs. Time plot, where effective predictions would lie on the ground truth RUL line (black solid line) for all times. The red dots in the plots represent predicted performance at times when the Bayesian updating was applied. Error bars represent the spread of predicted PDF for corresponding prediction. The validation of the proposed prognostic method is given in Fig. 19.

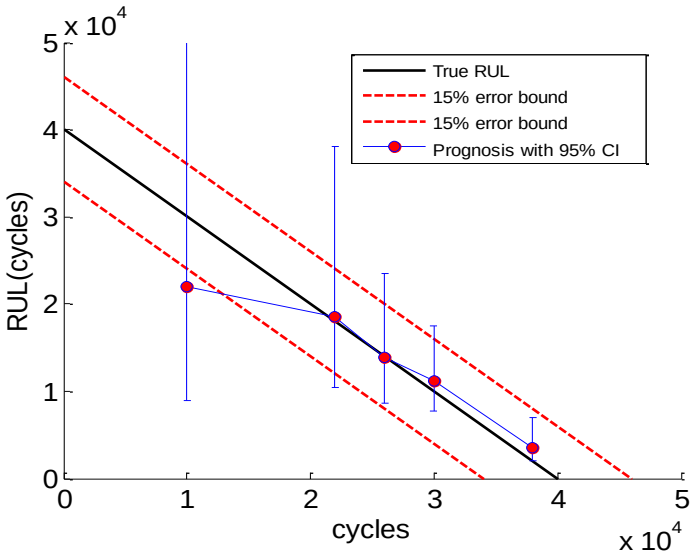

Fig. 19. Prognostic performance assessment

Fig. 19 shows that the excellent median prediction illustrated as pink dot is obtained after each updating. The proposed prognostic method can provide effective median RUL prediction when prognosis horizon (PH) is about 2×10^4 cycles and the 95% RUL prediction interval enters the 15% error bound at the fourth updating.

6. Conclusions

In this paper, an integrated fatigue damage diagnostics and prognostics methodology is proposed, which combines a piezoelectric sensor network-based damage detection method, data-driven stiffness degradation model in a Bayesian updating framework. The proposed method is demonstrated and validated using open-hole specimen datasets. Finally, the model predictions are evaluated using prognostic metric quantitatively. Based on the results obtained, several conclusions can be drawn:

1. Three stages of stiffness degradation are observed from the experimental testing results. The degradation rate is not monotonic and decreases initially and increases later;
2. The stiffness degradation rate is shown to be dependent on the current stiffness value and applied loading. A power law stiffness degradation model is proposed to consider the stiffness degradation and is shown to provide satisfactory predictions for the fatigue life;
3. The remaining useful life of composite specimen is negligible when the stiffness is below 0.75 of the virgin material stiffness in the current study;
4. Single feature from piezoelectric sensor is not able to correlates with the stiffness degradation in the current testing and multiple features need to be combined to reduce the estimation uncertainties. 90% probability of detection when the normalized stiffness is less than 0.97 is achieved using the proposed feature integration model;
5. Bayesian updating with the estimated stiffness degradation from piezoelectric sensor can greatly reduce the prognosis uncertainties as more measurements are available.

Only constant loading spectrum is used in this study. The composites stiffness degradation under variable amplitude loading should be explored for future studies. Stiffness degradation and damage detection using other SHM/NDT techniques, such as thermography, X-ray diffraction

imaging, and ultrasound scanning, will need more investigation. A multi-modality damage diagnosis framework may be able to further reduce the prediction uncertainties. Physics-based models will need further investigation to couple the different types of damage and damage detection simulation for integrated diagnosis and prognosis of composite materials.

Acknowledgement

The research reported in this paper was partially supported by the NASA through Global Engineering and Materials, Inc. (GEM) under the project NNX12CA86C. The support is gratefully acknowledged.

References

1.Choi N-S, Takahashi K,Hoshino K. *Characteristics of acoustic emission during the damage process in notched short-fibre-reinforced thermoplastics.* NDT & E International 1992; **25**(6):271-278.
2.Hallett SR, Green BG, Jiang WG,Wisnom MR. *An experimental and numerical investigation into the damage mechanisms in notched composites.* Composites Part A 2009; **40**(5):613-624.
3.Mallick PK. *Effects of hole stress concentration and its mitigation on the tensile strength of sheet moulding compound (SMC-R50) composites.* Composites 1988; **19**(4):283-287.
4.Yudhanto A, Iwahori Y, Watanabe N,Hoshi H. *Open hole fatigue characteristics and damage growth of stitched plain weave carbon/epoxy laminates.* Int J Fatigue 2012; **43**:12-22.
5.McNulty JC, He MY,Zok FW. *Notch sensitivity of fatigue life in a Sylramic TM/SiC composite at elevated temperature.* Compos Sci Technol 2001; **61**:1331–1338.
6.Nixon-Pearson OJ, Hallett SR, Harper PW,Kawashita LF. *Damage development in open-hole composite specimens in fatigue. Part 2: Numerical modelling.* Compos Struct 2013; **106**(0):890-898.
7.Nixon-Pearson OJ, Hallett SR, Withers PJ,Rouse J. *Damage development in open-hole composite specimens in fatigue. Part 1: Experimental investigation.* Compos Struct 2013; **106**(0):882-889.
8.RINDERKNECHT S,KROPLIN B. *A finite element model for delamination in composite plates.* Mech Compos Mater Struct 2007; **2**(1):19-47.
9.Keshava Kumar S, Ganguli R,Harursampath D. *Partial delamination modeling in composite beams using a finite element method.* Finite Elem Anal Des 2013; **76**(0):1-12.
10.Zhang J, Liu K, Luo C,Chattopadhyay A. *Crack initiation and fatigue life prediction on aluminum lug joints using statistical volume element-based multiscale modeling.* J Intell Mater Syst Struct 2013; **24**(17).
11.Zhang J, Johnston J,Chattopadhyay A. *Physics-based multiscale damage criterior for fatigue crack prediction in aluminum alloy.* Fatigue Fract Eng M 2014; **37**(2):119-131.
12.Hosseini-Toudeshky H, Jahanmardi M,Goodarzi MS. *Progressive debonding analysis of composite blade root joint of wind turbines under fatigue loading.* Compos Struct 2015; **120**:417-427.
13.Hosseini-Toudeshky H, Jasemzadeh A,Mohammadi B. *Fatigue debonding analysis of repaired aluminium panels by composite patch using interface elements.* Appl Compos Mater 2011; **18**(6):571-584.

14.Mazaherial F,Hosseini-Toudeshky H. *Low-cycle fatigue delamination initiation and propagation in fibre metal laminates.* Fatigue Fract Eng M 2014; **DOI: 10.1111/ffe.**
15.Hossein H-T, Goodarzi MS,Mohammadi B. *Prediction of through the width delamination growth in post-buckled laminates under fatigue loading using decohesive law.* Struct Eng Mech 2013; **48**(1):41-56.
16.Highsmith A,Reifsnider KL. *Stiffness reduction mechanisms in composite laminates.* In: Reifsnider KL, editor. Damage in Composite Materials. American Society for Testing and Materials 1982; **775**:103-117.
17.Philippidis TP,Vassilopoulos AP. *Fatigue design allowable for GRP laminates based on stiffness degradation measurements* Compos Sci Technol 2000; **60**:2819-2828.
18.Agarwal BD,Joneja SK. *Flexural fatigue properties of Unidirectional GRP in the transverse direction.* Composites 1979; **10**(1):28-30.
19.Ambu R, Aymerich F,Bertolino F. *Investigation of the effect of damage on the strength of notched composite laminates by digital image correlation.* J Strain Anal Eng Des 2005; **40**(5):451-461.
20.Whitworth HA. *A stiffness degradation model for composite laminates under fatigue loading.* Compos Struct 1998; **40**(2):95-101.
21.Yang JN, Jones DL, Yang SH,Meskini A. *A stiffness degradation model for Graphite/Epoxy laminates.* J Compos Mater 1990; **24**:753-769.
22.Shirazi A,Varvani-Farahani A. *A Stiffness Degradation Based Fatigue Damage Model for FRP Composites of (0/ϑ) Laminate Systems.* Applied Composite Materials 2010; **17**:137-150.
23.Lemistre M,Balageas D. *Structural health monitoring system based on diffracted Lamb wave analysis by multiresolution processing.* Smart Mater Struct 2001; **10**:504 doi:10.1088/0964-1726/10/3/312.
24.Giurgiutiu V, Zagrai A,Bao JJ. *Piezoelectric wafer embedded active sensors for aging aircraft structural health monitoring.* Struct Health Monit 2002; **1**(1):41-61.
25.Constantin N, Sorohan S,Gavan M. *Efficient and low cost PZT network for detection and localizaiton of damage in low curvature panels.* Journal of Theoretical and Applied Mechanics 2011; **49**(3):685-704.
26.Scalea d, Francesco L, Robinson JS, Tuzzeo D,Bonomo M. *Guided wave ultrasonics for NDE of aging aircraft components* Proc SPIE 2002; **4704**:123-32.
27.Press S. *Subjective and objective Bayesian statistics: principles, models, and applications.* Wiley-Interscience, Hoboken, NJ 2003.
28.Caticha A,Giffin A. *"Updating probabilities" in Bayesian Inference and Maximum Entropy Methods in Science and Engineering.* AIP Conference Proceedings 2007; **872**:31.
29.Peng T, Saxena A, Goebel K, Xiang Y, Sankararaman S,Liu Y. *A novel Bayesian imaging method for probabilistic delamination detection of composite materials.* Smart Mater Struct 2013; **22**(12):125019.
30.Peng T, He J, Xiang Y, Liu Y, Saxena A, Celaya J,Goebel K. *Probabilistic fatigue damage prognosis of lap joint using Bayesian updating.* J Intell Mater Syst Struct 2014; **1045389X14538328**.
31.Adam MT. *G104-A2L Guide for estimation of measurement uncertainty in testing.* American Association for Laboratory Accreditation, 2002. p.10-18.
32.Bell S. *A beginner's guide to uncertainty of measurement.* The National Physical Laboratory 2001; **2**:9-16.
33.Cowles MK,Carlin BP. *Markov Chain Monte Carlo convergence diagnostics: A comparative review.* J Amer Statist Assoc 1996; **91**(434):883-904.
34.Fort G, Moulines E,Priouret P. *Convergence of adaptive and interacting Markov Chain Monte Carlo algorithms.* Ann Stat 2012; **39**(6):3262-3289.

35.Hasting WK. *Monte Carlo sampling methods using Markov Chain and their applications.* Biometrika 1970; **57**:97-109.
36.Peskun PH. *Aptimum Monte Carlo sampling using Markov chains.* Biometrika 1973; **57**:97-109.
37.He J, Guan X, Peng T, Liu Y, Saxena A, Celaya J,Goebel K. *A multi-feature integration method for fatigue crack detection and crack length estimation in riveted lap joints using Lamb waves* Smart Mater Struct 2013; **22**(10):105007.
38.Kurz JH, Jüngert A, Dugan S, Dobmann G,Boller C. *Reliability considerations of NDT by probability of detection (POD) determination using ultrasound phased array.* Eng Fail Anal 2013; **35**(0):609-617.
39.*ASTM E647-13ae1, Standard Test Method for Measurement of Fatigue Crack Growth Rates, ASTM International, West Conshohocken, PA, 2013, www.astm.org.*
40.Saxena A, Celaya J, Balaban E, Goebel K, Saha B, Saha S,Schwabacher M. *Metrics for evaluating performance of prognostic techniques.* Prognostics and Health Management, Denver, CO, 2008. p.1-17.
41.Guan X, Liu Y, Jha R, Saxena A, Celaya J,Goebel K. *Comparison of two probabilistic fatigue damage assessment approaches using prognostic performance metrics.* International Journal of Prognositics and Health Management 2011; **2**(1):11.
42.Saxena A, Celaya J, Saha B, Saha S,Goebel K. *Uncertainty quantification in fatigue crack growth prognosis.* International Journal of Prognositics and Health Management 2011; **2**(1):15.
43.Saxena A, Celaya J, Saha B, Saha S,Goebel K. *Metrics for offline evaluation of prognostic performance.* International Journal of Prognositics and Health Management 2010; **1**(1):20.